Swartz, M., G.Verner, A.Weinberg, "Non-Thermal Near-IR Emission from High Impedance and Codeposition LANR Devices", Proceedings ICCF-14, ISBN: 978-0-578-06694-3, 343, (2010).

Non-Thermal Near-IR Emission from High Impedance and Codeposition LANR Devices

Mitchell Swartz, Gayle Verner, Alan Weinberg
JET Energy, Inc. Wellesley, MA 02481(USA)

Abstract:
Near-IR radiation is emitted from lattice assisted nuclear reactions [LANR] during their excess heat operation. The appearance of anomalous amounts of heat in shaped high impedance and codeposition was simultaneously detected from loaded, active nickel and palladium LANR systems ($Pd/D_2O/Pt$,$Pd/D_2O/Au$, Ni/H_2O_{1-x},D_2O_x/Pt, Ni/H_2O_{1-x},D_2O_x/Au], and some codepositional [$Pd/Pd(OD)_2/Pt$], by in situ monitoring. LANR devices was simultaneously detected when they were driven at their optimal operating point. This near IR emission be non-thermal (NT-NIR) because it appears to be linked to, and specific for, an active LANR devices' excess heat production and not its physical temperature. This began as an attempt to improve Szpak's et al. findings with a control. We have found that as a minimum, two controls are needed for examining IR images; thermal controls must be augmented by spatial controls. These findings of NT-NIR may confirm the Bremsstrahlung-shift hypothesis that with low temperature fusion, there is a temperature-controlled shift from penetrating ionizing radiation to skin-depth-locked infrared radiation.
Keyword - lattice assisted nuclear reactions; near IR emission; palladium; Bremsstrahlung

1.1 Introduction – Lattice Assisted Nuclear Reactions

In this paper, we report that localized hot spots develop, revealed by near infrared imaging associated with excess heat in active LANR devices [Figure 1].

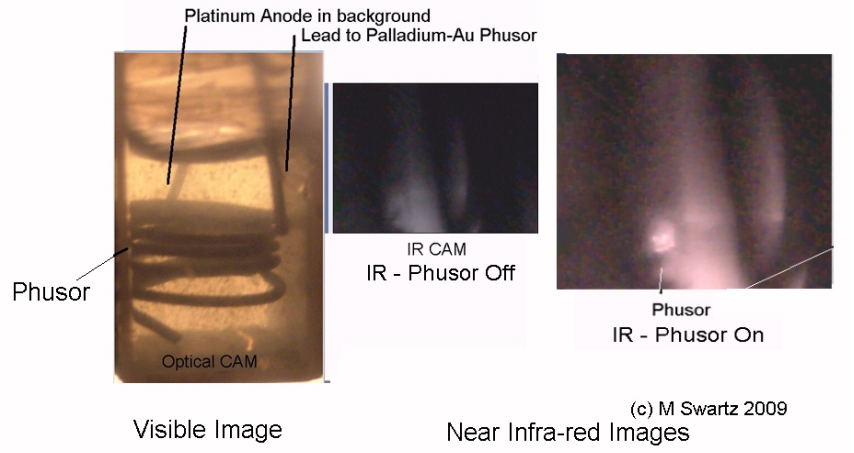

Figure 1 -Visible and Near-IR Images of DAP LANR Cell Before and After Activation

Calibrated imaging has indicated that this is non-thermal near-IR (NT-NIR) emission linked, and specific, to the presence of excess heat production and not necessarily physical temperature [Figure 2]. These findings, including those shown in Figures 1 and 2 may confirm the Bremsstrahlung-shift hypothesis that in LANR, unlike hot fusion, Bremsstrahlung emission, under increasingly lower temperatures, shifts from penetrating ionizing radiation toward skin-depth-locked infra-red radiation [Swartz 1999b].

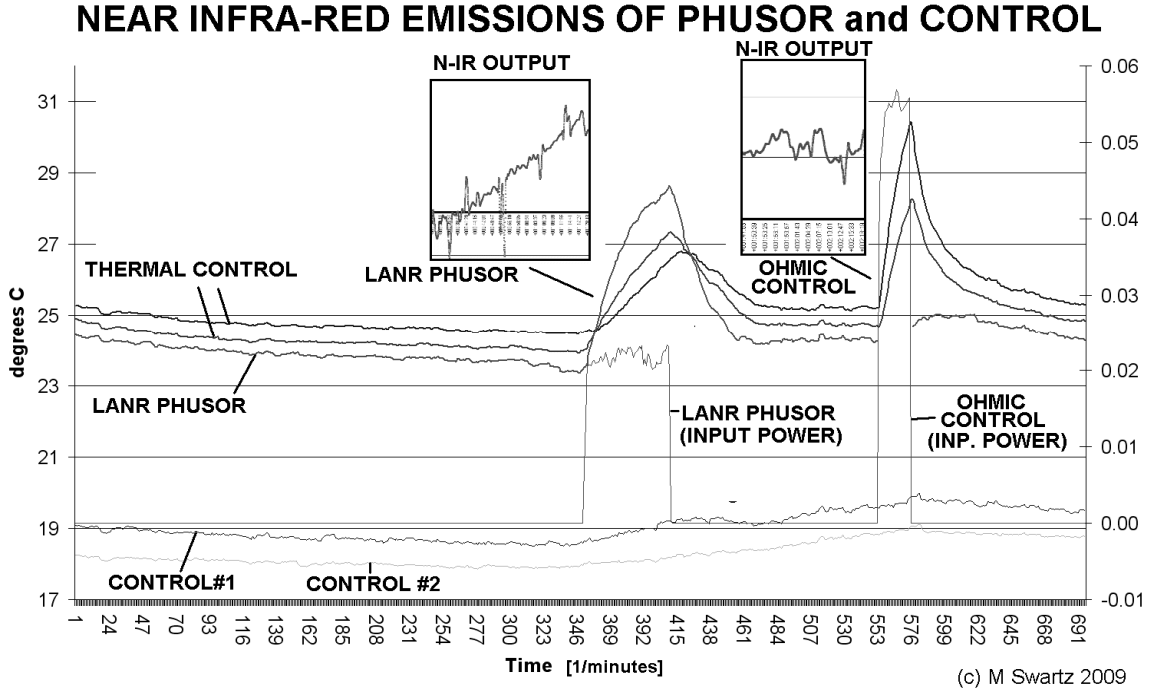

Figure 2 – Thermometry and Non-thermal Near-IR Emission from DAP LANR device.

1.2 Background – LANR Nuclear Physics and Electrical Engineering

Lattice assisted nuclear reactions [LANR] are real and generated in deuteron-loaded, metallic palladium, PdD_x, and other metals [Fleischmann 1989; Pons 1994; Swartz 1997a,1997b, 2005, 2006a, 2008, 1998a, 2006b, 2002, 2009a; Szpak 1991, 1992, 1994a, 2004, 1995, 1996;1998, 1996, 2007; Mosier-Boss 1999; 2007, 2009; Szpak 2005, 2005; Arata 1999; Dardik 2003; Case 1998; Letts 2003; McKubre 2003; Miles 1993; Srinivasan 1992; Violante 2003; Will 1993; Dash 2007; Stringham 2003; Iwamura 2002; Letts 2008; Li 1990; Miley 2005; Takahashi 2008; Swartz 2000a, 1999a, 1998b, 2008, 1994a, 1992, 2000b, 1997c, 1998c, 1996]. In LANR systems and devices, the fuel is the deuteron, driven into the metal by the applied electric field intensity or by gas pressure applied. The fuel is obtained either from deuterons from heavy water or gaseous deuterium. In most cases, the dominant reaction product is an extraordinary amount of heat associated with commensurate amounts of *de novo* helium-4 [Melvin Miles, China Lake, Johnson-Matthey Pd rods; requiring metal flasks; Miles 1993]

The observed excess heat in LANR is energy and momentum transferred to its lattice, as they are conserved [Hagelstein 2008, 1993; Swartz 1997d; Rabinowitz 1993; Swartz 1994b; Chubb 1994; Kim 2008]. Because of the unique relationship to the lattice [Gibb 1974; Dickson 1983; Gonser 1975; Swartz 2009c], the LANR-generated helium is moving slowly, at low velocity, very unlike hot fusion. The He^4 generated is retained in the cathode, until high temperatures (~850C; Arata and Zhang).

In 1989, P-F reported excess energies of 4 MJ (megajoules) in 80 hours. The energy density was circa 7 W/cm^3. Today, this has increased to circa 1000 W/cm3 or more, with Italian reports of ~40,000 W/cm^3 for wire configurations. This amount of excess energy

brings substantial ("excess") heat and sometime disruptive changes wrought upon the electrode. SPAWAR, JWK, Stringham, Dash and others have reported volcano looking pits in electrodes. These induced pits are important for two reasons. First, they demonstrate substantial energy was generated producing focal melting of the Pd. Second, this amount of energy corroborates that LANR energy is from a nuclear source, since the excess energy observed is greater than any known chemical reaction. Even if one were to replace the entire cathode with TNT, one would only get 1.2 KJ (kilojoules) maximum.

Today, several varieties of LANR devices/systems show excess power gains varying from 125% to 180%, with high impedance LANR devices exhibiting power gains of 200% to ~8000%,. In 2003, a LANR high impedance Phusor®-type LANR system ran continuously for five days at MIT at ICCF10, producing ~230% excess energy at 1 to 2 watt level, with public demonstration of optimal operating points. Under some conditions, more robust LANR systems can yield significant excess heat, driving motors and producing electricity, with peak excess power production levels successfully driving Stirling engines at the 1-19+ watt level [Swartz 2009b,1997a, 2005, 2006a; Letts 2008; Swartz 1998, 2002].

Under some conditions, tritium and other emissions result, including charged particles, and a very low number of neutrons. In India, M. Srinivasan from the (BARC) reported tritium in 1989. John Bockris (Texas A&M) reported tritium in bursts but the tritium was not accompanied by measurable heat. Szpak (SPAWAR) reported 3000 to 7000 atoms per second for a 24 hour period. Ed Storms (LANL) reported excess tritium in ten percent of his cells. M. Srinivasan (BARC) reported neutrons in 1989. As the current increased beyond 100 amperes, neutron signals, in bursts, resulted in six of 11 cells. X.Z.Li (Tsinghua U) first used CR-39 in his 1990 Pd gas loading experiments to detect energetic charged particles [Swartz 1994b]. CR-39 is a polyallydiglycol carbonate polymer, widely used as a time-integrating, solid state, nuclear track detector. Larry Forsley (JWK International) and Mosier-Boss (SPAWAR) greatly developed this, and have reported D-D and D-T possible reaction pathways capable of generating the observed charged particles, neutrons, etc. Their CR-39 tracks indicate possible neutron interactions, including carbon shattering. Some tracks herald D-D and DT reactions. Etching suggests uniformity in the 2-8 MeV range. The triple tracks, found in ~5-10 of their experiments, indicate rare energetic neutrons and rarer secondary shattered carbon atom.

Other LANR emissions include soft penetrating, ionizing radiation. Miles (China Lake, USN) and M. Srinivasan (Bhabha Atomic Research Center, BARC) independently used dental x-ray films on the outside of his apparatus; they became fogged indicating low energy x-ray production.

There appears to be more than one LANR location, each characterized by its own rate of excess heat, tritium, and helium production, and each linked to a different optimal operating point [OOP] manifold [Dash 2007; Li 1990; Miley 2005; Takahashi 2008; Swartz 2000a, 1999a]. There are other difficulties, like hot fusion, which include containment, time, and density. However, deuteron flux is more important in LANR than temperature [Swartz 2009a, 2000a, 1999a,1998b, 2008,1994a, 1992, 2000b, 1997c,

1998b]. The PdD_x alloy must be driven to extremely high loading, until almost bursting. Loading must exceed >90%, and incubation times are on the several hundreds of hours as vacancies are presently believed to drift into the bulk from the surface, slightly facilitated by the loading itself [Swartz 2009b, 2006a 2009c]. The most important point is that these observations of significant "excess" heat, mini-explosions, ionizing radiation, high energy charged particles, tritium and neutron production, are accumulating forensic evidence which support the fact that nuclear reactions occur in, and are assisted by, a lattice, and they can be initiated by low energy activation.

1.3 Background – Types of LANR Engineered Systems

Increasing power gains and total energies been achieved since 1989 through two decades of R&D, sub rosa. Today, there are several types of LANR; conventional (F+P), two types of codeposition (JET Energy, SPAWAR), dual cathode (Arata) systems, and a variety of other loading systems. LANR loading systems include electric, gas loading, gas permeation, ion beam and glow discharge loading techniques and devices. They run in both open and closed systems, at pressures up to 10,000 psi, and driving motors, with on-line monitoring, redundant, high precision, time-resolved semiquantitative calorimetry.

On one hand, development for high power has led to today's high electrical solution resistivity LANR systems (very low levels of electrolysis yield superior excess heat levels pioneered by JET Energy) and then LANR metamaterials [Swartz 2009a]. We have shown that some electrodes, of specific shape, are metamaterials which produce excess heat of a superlative magnitude. These metamaterials use shapes engineered to control deuteron flux, even at equilibrium, and even after loading. Some of these exhibit impressive energy gain and fairly good reproducibility. Using low electrical conductivity D_2O with platinum or gold anodes, they can generate excess heat beyond thermal controls in careful precise experiments. The Phusor® type spiral cathode system, with its open helical cylindrical geometry, in a high electrical resistance solution, creates a unique and unusual electric field distribution [Swartz 2009a]. There is an anomalous effect in those portions of the cathode closest to the anode. This results in both deuteron loading flux from the solution to the electrode, and intra-palladium deuteron flux [Swartz 2009a, 1994a, 1992]. These configuration include several types of nickel and palladium high electrical impedance Phusor [$Pd/D_2O/Pt$,$Pd/D_2O/Au$, $Ni/H_2O_{1-x},D_2O_x/Pt$, $Ni/H_2O_{1-x},D_2O_x/Au$], and some codepositional DAP-Phusor [$Pd/Pd(OD)_2/Pt$] devices and associated driving systems (active volumes ~0.47 cm^3, loading surface area ~6.4 cm2) [Swartz 2009b, 2006a]. These contain low paramagnetic content heavy water creating a unique, distinguishing electric field distribution quite different from customary wire-wire and plate-plate systems. LANR metamaterials, and high loading systems (included those explored by IENA, Energetics) and metallurgically engineered electrodes (NRL, SPAWAR, JET Energy) all point the way to high output powers and efficiencies.

On the other hand, codeposition LANR systems yield speedy onset for some of the reactions, with faster loading times within minutes, without the prolonged incubation times. Codeposition may also have higher repeatability for some LANR processes. In codeposition systems, fresh Pd and D plate out together on the cathode. Highly expanded

surfaces, nanoscale spherical nodules dominate on the growing surface. Cyclic voltammetry and galvanostatic pulsing experiments indicate, and excess heat measurements herald, that a high degree of deuterium loading (with an atomic ratio D/Pd>1) is obtained within seconds (SPAWAR). The results to date indicate nuclear reactions occur very near the surface of the electrode (within a few atomic layers).

In the original JET Energy Pd/D codeposition process, working and counter electrodes are immersed in a solution of palladium solution with neither chloride nor lithium, deposited on palladium. In the SPAWAR Pd/D codeposition process, working and counter electrodes are immersed in a solution of palladium chloride and lithium chloride in deuterated water, deposited onto silver, gold, or copper. There are physical differences in the two types involving deep diffusion [Swartz 1997b], where Pd is deposited either on palladium (like Dr. Swartz) or upon non-loading materials such as copper, gold, silver, or platinum (like SPAWAR).

1.4 Background – Optimal operating point (OOP) Operation of LANR

We have found that anomalous energy gain in metal deuterides has become a much more reproducible phenomenon with OOP control, and with false positives ruled out by noise measurement, adequate Nyquist sampling, time-integration, and thermal waveform reconstruction with several types of joule, thermal and other controls. OOPs explain a vast set of experimental LANR data, not otherwise explicable. When LANR product output data is viewed along the electrical input power axis, the OOPs are the peaks of each of these, some relatively narrow, biphasic functions which represent the excess heat generation, and peak helium-4 or tritium production (Figure 3).

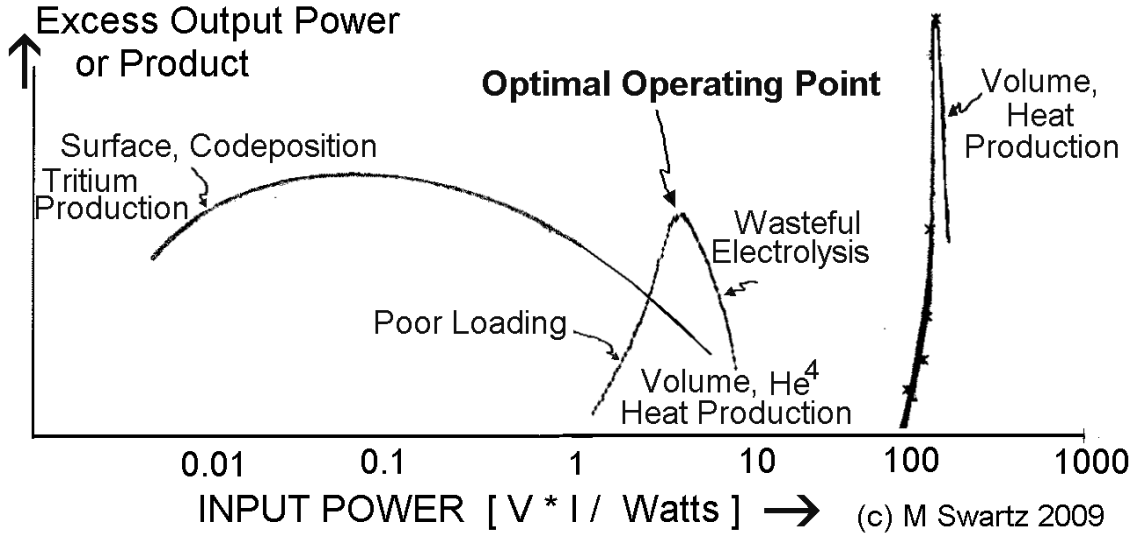

Figure 3 – Three LANR Optimal operating point (OOP) manifolds

Figure 3 shows three OOP manifolds for LANR systems representing excess power gain, de novo helium[4] and tritium production, for conventional, high-impedance, codeposition and palladium-black nanomaterial LANR systems. Large changes in LANR output are observed as the input power is varied over a relatively small range. Attention is directed

to the fact that when LANR data is thus organized, it formidably dispels any arguments that LANR research is not reproducible.

The OOP peak is only one operating point at which the LANR system can be driven. The other possible operating points at which the system can be driven, are not "optimal", but are within the OOP manifold. In OOP-controlled LANR the samples or devices are driven at their optimum operating point for peak excess heat production points along the input electrical power axis, where the likelihood of desired output is maximized. Over the years, the optimal operating point (OOP) approach to LANR has been quite successful [JET Energy (Swartz 2000a, 1999a, 1998b, 2008, 1994a, 1992, 2000b, 1997c, 1998b); JWK (Swartz 2009); Innoventek (Bass 2008)]. OOP operation enables researchers to 'standardize' samples and devices, which has lead to several discoveries, including those which only occur when the LANR sample or device is driven at the OOP. This includes maximizing and controlling "heat after death", the response to incident coherent optical radiation, and producing non-thermal near IR emission. The development of optimal operating point (OOP) technology has been one of our most useful assets in this research.

1.5 Background – IR Observations in LANR

Dr. Stan Szpak (SPAWAR) *et alia* reported the emission of infra-red from LANR codeposition devices. However, they did not use a control, and there have been questions concerning both the linearity and calibration of their single effort. That led to this report made to answer the question: Would there be near-IR emission from a Phusor®-type LANR Device during its production of excess heat? Could it be confirmed by simultaneous calorimetry and heat flow measurements while calibrated against an ohmic joule control?

SPAWAR and JET have investigated the physical changes, the excess heat generation, hot spots with calibration showing near and, and with this paper, far IR emission (Figure 1). JET Energy and SPAWAR have revealed, using near- and medical IR imaging respectively, that in LANR there are cathodic hot spots, and not just Joule heating in the solution (IR drop). The desired reactions producing excess energy yield localized hot spots (Szpak). JET Energy has examined the impact of laser irradiation on LANR cathodes, and reported in 2003 that part of the impact is due to reflection off of the cathode back into the double layer. There, deuteron injection into the palladium increases (activation energy of ~14 kilocalories per mole) from microwave rotation and IR vibration for the intermolecular transfer of deuterons to the Pd [Swartz 2006b]. Hagelstein, Letts and Cravens [Letts 2003, 2008] have reported both single and dual photon impacts on cathodes.

2.1 EXPERIMENTAL – Materials

The cathodes were cold-worked spiral wound Phusor®-type LANR palladium cathodes [wire, 99.98+%, Alfa Aesar, Ward Hill, MA, 1.0 mm diameter, number of turns ~4-7, spiral 13 mm diameter, gap separation from the anode of 6 mm, total mass 3.26 grams] arranged in a Pd/D_2O/Pt or Pd/D_2O/Au configuration. The cathodes had four leads attached, for four terminal electrical conductivity measurements. The anodes were platinum or gold wire [1 mm diameter, 99.998].

Both electrodes were immersed in very low electrical conductivity D_2O with no additional electrolyte. The low electrical conductivity water bathed the spiral cathode. The solution is very low electrical conductivity heavy water [deuterium oxide, low paramagnetic, 99.99%, Cambridge Isotope Laboratories, Andover MA] to minimize unwanted reactions of electrolysis. The volume of the heavy water solutions in the various calorimeters (see below) ranged from 10-60 cubic centimeters, usually ~30-40 cm3. Additional isolated volumes of light (ordinary) water were used for the multiring calorimeter but were only in thermal contact with the heavy water. The heavy water is hygroscopic, therefore kept physically isolated from the air by seals, including several layers of Parafilm M [American National Can, Menasha, WI] and paraffin. We continue to avoid chlorine or chloride because of possible explosions. This is due to visible light ignition-susceptibility because the activation energy required is ~17 microjoules.

Polyethylene and polypropylene walled paraffin-sealed containers held the heavy water, electrodes, and temperature probes, and for connections for position, when possible. Neither silicates nor glasses were used in the inner chamber. Materials used in construction included medical grade polyethylene and polypropylene. All leads near the solution were covered with electrically-insulating tubes (medical grade silicone or Teflon) used to electrically isolate wires. For support, acrylic, Styrofoam, and wood were used for their low thermal conductivity, and thus thermal isolation. Here, we wanted to do simultaneous in situ imaging (near-IR and visible). The experiments were conducted using in situ imaging (near-IR and visible) in a dual adjacent calorimeter, supplementing other diagnostics. A rhomboidal near-transparent holding cell, appropriate for the heavy water, diagnostics, thermal sensing devices, dual anodes, and palladium cathode, was designed based on two near identical containers adjacent to each other.

Contamination remains a major problem, with excess heat devastatingly quenched by increasing electrical conductance of the solution [Swartz 2006a] and effects on the cathode. Contaminants appear from both electrode and container degradation and leeching, from atmospheric contamination, and after temperature cycling. These all inexorably, unintentionally, add to the electrolytic solution decreasing the level of deuteron loading achieved, the rate of loading as well, and the maximum heat producing activity.

2.2 EXPERIMENTAL – Methods – Electrical Loading and Preparation

The loading of the palladium from the heavy water, and driving of the reactions through the two electrodes within the reaction container was obtained by both electric current and electric voltage sources. Electrical ccurrent sources included Keithley 225, HP 6177c, with outputs +/-1% accuracy. Electrical voltage sources included LAMBDA 340A, HP722AR, HP/Harrison 6525A, Nobatron DCR-150, and Fluke 412B to obtain transsample potentials up to 3000 volts [~+/-0.5% accuracy]. All connections were checked with computer and/or Keithley 610C, Keithley 160B, 178, 179, Dana Electronics 5900, or Fluke 8350A meters. When possible, Keithley electrometers were used for computer isolation. All leads near the solution were covered with electrically-insulating

tubes (medical grade silicone, Teflon, or proprietary materials) used to electrically isolate wires. Impedances of all leads were measured, and included in the derivation of all corrected values. For 4-terminal intra-electrode Palladium electrical conductivity measurements, a first Keithley 225 electric current source was used to drive the cell, and load the Phusor. A second Keithley 225 electric current source was used to drive the electrical current portion of the four terminal electrical conductivity measurement of the palladium.

The data from voltage, current, temperatures at multiple sites of the solution, and outside of the cell, the 4-terminal measurement of the cathode's internal electrical conductivity, additional calibration thermometry and other measurements were sampled at 0.20 Hertz, usually 1 Hertz, to 22 bits resolution (Omega OMB-DaqTemp (Omega; voltage accuracy 0.015+/-0.005 volts, temperature accuracy <0.6 degrees C) and recorded by computed DAQ. To minimize quantization noise, 1 minute moving averages were sometimes made. The noise power of the calorimeter is in the range of ~1 to 30 milliwatts. The noise power of the Keithley current sources is ~10 nanowatts.

Input power was defined as V*I. There is no thermo-neutral correction in denominator. Therefore, the observed power is a lower limit because the thermoneutral potential is usually subtracted from the denominator, but is not used here. The instantaneous power gain [power amplification factor(non-dimensional)] is defined as Pout/Pin, as calibrated by at least one electrical joule control [ohmic resistor] and time integrated for validation. The excess energy, when present, is defined as [Poutput - Pinput] * time. The amount of output energy is interfered from the heat released producing a temperature rise, which is then compared to the input energy.

For the codepositional DAP (Dual anode Phusor®-Type LANR device; [Pd/D_2O, $Pd(OD)_2$/Pt-Au]). The goal was to set up an optimal heat-generating binary or ternary alloy cathodic surface that would contain, upon its bed of palladium, the requisite materials and composition for high loading and successful LANR. Palladium was used at the start as a fraction of the sacrificial anode (2.01g) was corroded in order to generate the desired codeposition solution, for improved loading, and to lay down a palladium nanostructure upon the surface of a virgin palladium cathode. Then, the palladium anode was removed, and was replaced by a gold wire anode in order to stop the addition of further codeposition solution, and to stop the laying down of further palladium nanostructure upon the palladium cathode. This result is a Pd*/D_2O-$Pd(OD)_2$/Au Phusor®-type cathode.

The initial codeposition decreases the cell resistance from 868 kilohms down to 48.3 kilohms, and if continued beyond, to ~2500 ohms and less. Prior to all depositions, the open circuit voltage, V_{oc}, of the two virgin palladium pieces prior to the start of the experiment was -15.5 to -21.4 millivolts. Using a complicated proprietary driving system, we electrodeposited the requisite materials to the solution and surface of the cathode, the estimated layer of Pd on the surface was circa 17,000 atoms deep, with a solution of 7.7 millimolar $Pd(OD)_2$ in the solution. The open circuit voltage, V_{oc}, at the end of surface preparation, was 1.46 volts.

2.3 EXPERIMENTAL – Thermometry and Calorimetry

Temperature measurements were made by electrically-insulated thermocouples [accuracy +/-0.8 deg.K, precision +/-0.1 deg.K], RTD and other sensors. Probes were calibrated by Omega IcePoint Cell. Core temperatures were maintained by feedback control using a Yellow Spring Thermal Controller Model 72 [bandwidth of 0.2 K] within a Honeywell water circulation zone controlled room (+/- 2.5 degrees K). Thermocouples and other temperature sensors decorated the periphery of the cell, and a multicompartment calorimeter was used. There was an additional heat-flow probes at the periphery outside of the core. To minimize contamination, the majority of temperature measurements were outside of the inner core container.

Calorimetry evaluated and verified active LANR behavior using redundant calorimetry, heat flow measurement, electricity production using thermoelectrics. We used several corroboratory measurements, different methods to evaluate the presence, if any, of excess heat, including redundant calorimetry and heat flow sensors. Each output was normalized to input electrical power, and also calibrated by ohmic (thermal) controls, to evaluate, and certify possible anomalous heat. Additional calibration has included adequate Nyquist sampling, time-integration, thermal ohmic controls, waveform reconstruction, noise measurement, and other techniques [Swartz 2009b,1997a, 2006a, 2005].

Because of potential errors and negative effects on system performance associated with flow calorimetric systems, we have developed several types of modified multiring calorimeters [Swartz 1997a]. These calorimeters have redundant thermometry, checked by thermal waveform reconstruction and thermal controls. In this case, the thermal (ohmic resistor) control used as a joule control and non-loading heater, and to calibrate the system both for input electrical power and to make other checks including square-wave reproducibility, and time invariance, was carefully hermetically protected from the heavy water by polypropylene or other material and immersed in water. The resistor was chosen to have an impedance close to the expected solution resistance in the LANR system, often several to tens of thousands of ohms.

Information was obtained from these calorimeters, in part, using the difference between the core and the second ring temperatures, normalized by the input electrical power to determine the input-power normalized delta-T. This is compared to the ohmic control, and also checked by independent calorimetric systems and by a heat flow measurement. In this system, the foreground data is obtained when an electric field intensity is applied to the LANR device producing entry of heavy hydrogen from the heavy water into palladium electrode, and a deuterium flux through the electrode. The background data is obtained when an electric square wave current pulse was applied to the resistor's leads as the control, for heat calibration.

2.4 EXPERIMENTAL – Methods - Near-IR Imaging

The goal here was to also add a thermal control, while driving the active LANR device's excess heat at its optimal operating point. Limited by funding and time constraints, we

have built several custom in situ LANR imaging systems for near infrared (NIR). This study was at a different wavelength than the preliminary thermal IR results from Dr. Szpak. We sought to use in situ imaging of LANR devices in both the near-infrared (NIR) and the visible region. Such multiband imaging with simultaneous precision calorimetry has been challenging, requiring careful spatial and thermal calibrations not only of the devices, but also both ohmic controls and the environment. Several LANR devices were designed. The best used very thin, rhomboidal near-transparent cells built into multiring calorimeters.

We incorrectly thought a single control (vs. Szpak et al who had used no controls) would be needed. It was soon discovered that two controls are needed. Thereafter, calibration included normalization of NIR emission intensities to both non-energized environmental and to ohmic control areas. The derived IR output information, during active LANR state calorimetry, was initially semiquantitatively calibrated against an ohmic thermal control. However, it was determined that two controls are needed for examining IR images, so thermal controls as before, had to be augmented by spatial controls, initially unanticipated. NIR information, obtained by semiquantitative correction using two simultaneous control measurements, while accompanied by precision OOP-controlled calorimetry during the high voltage driving of the LANR system, has been challenging. It was assisted by calorimetry, diagnostics, imaging and data processing using several computers.

NIR data capture was by slow scan near-IR and visible videocam (~1 Hz). Thereafter information was obtained by analysis using semiquantitative computed measurements of collected NIR output, integrated over both the DAP cathode, the ohmic thermal control, and their environment as they were each activated or not. The integrated NIR output of serial computed images of the DAP Phusor® and ohmic control were compared by normalization to the controls, and examined as a function of time (as shown in Figure 2). Matched arrays of solar cells integrated the recorded near-IR emissions of the DAP device, the thermal control, and the control areas over time. Centered over the Phusor® - type cathode and then the control area, these re-collected and integrated the NIR data as a single analog signals which were each digitized covering thousands of video images. Normalization to non-energized areas, and the control ohmic thermal area followed.

3.1 Results – DAP LANR Heat Results

The assembled cells had a dry (leakage) electrical resistance of ~10.6 megohms at 116 volts. Filled with pure heavy water, the wet electrical resistance of assembled LANR cells decreases during initial maturation and development. This has been discussed elsewhere for general high resistance type LANR devices where the cell's solution electrical resistance is ~95-200 kilohms. For these experiments, using DAP devices, the initial wet cell solution electrical resistance from 868 kilohms, which during processing decreased to 48.3 kilohms. At the end of its preparation, aided by proprietary loading means, the Pd*/D_2O-$Pd(OD)_2$/Au Dual Anode Phusor (DAP), had a Pd-D surface ~17,000 atoms deep. The solution was 7.73 millimolar $Pd(OD)_2$.

Excess power gain in most runs varied from circa 400%-800% based upon input power normalized delta-T measurements. The peak power gain was circa 8000% (Figure 4) which led to damage of the leads of the cell. The input power normalized delta-T curves are shown in Figure 4.

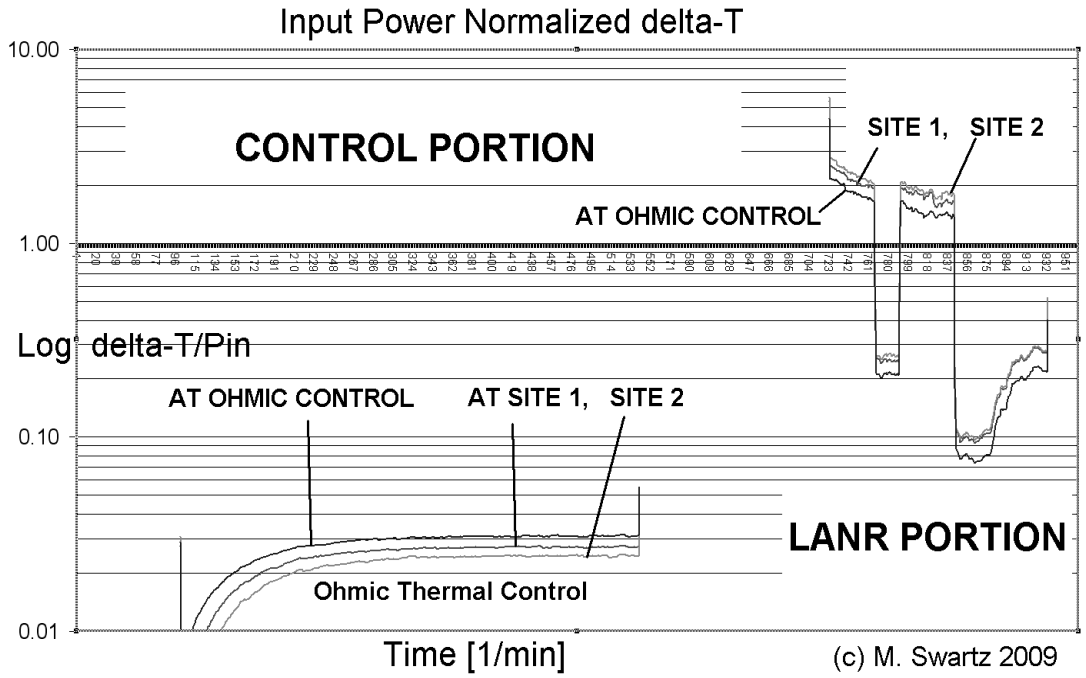

Figure 4 - Input power normalized delta-T curves for DAP Phusor® LANR

Imaging of Near-IR Emission from DAP codeposition

We report on the apparent linkage of excess power gain and excess heat flow with simultaneous non-thermal near-IR (NT-NIR) emission from a variety of LANR metamaterial spiral-wound and other Phusor®-type lattice assisted nuclear reaction (LANR) systems. Several types of such LANR devices were examined, including high impedance palladium [$Pd/D_2O/Pt$,$Pd/D_2O/Au$], codepositional [$Pd/Pd(OD)_2/Pt$] heavy water, and nickel [$Ni/H_2O_{1-x},D_2O_x/Pt$, $Ni/H_2O_{1-x},D_2O_x/Au$] light water Phusor-type LANR devices. Simultaneous excess heat and non-thermal near-infrared (NT-NIR) light emission has been detected from loaded, active palladium and some nickel Phusor-type LANR devices, by in situ monitoring (Figures 1 and 2).

The NIR image of the DAP Phusor® activated is on the right side of Figure 1. Figure 1 shows three views of a DAP codeposition Phusor®-Type LANR Device in heavy water, both before, and after, its activation and generation of excess heat. The first view is in ordinary light, the other two (from a slightly different angle of observation) are in the near infrared (NIR), both before and after the device's activation generating excess heat. The DAP Phusor® configuration was Pd/D_2O-$Pd(OD)_2$/Pt-Au using heavy water and ~7.7 millimolar $Pd(OD)_2$. This was arranged as an electrochemical cell within the inner compartment. The palladium cathode and palladium anode are seen before the start of any runs or measurements, as the control ("off"), on the left of Figure 1 as the visible image, and in the middle as the near-IR image. Portions of the DAP cathode are seen in

the heavy water cell. The platinum anode is seen in the background. The IR image of a Phusor activated on right. The Phusor is located in both images by a pointer. When activated, the DAP (Pd^*/D_2O-$Pd(OD)_2$/Au Dual Anode) Phusor®, the electrical current was 9 milliamperes during the imaging run. The peak voltage across the cell was 28.8 volts. The power gain was 182%, with 350 joules excess energy.

3.2 Results - Results - Non-thermal Near-IR Emission from DAP codeposition

Semiquantitative measurements with two controls reveal that the dynamic rise of NT-NIR emissions was only seen in the DAP Phusor during its activation and output of excess energy; and that NT-NIR emissions are linked, and specific, to the devices' excess heat production and not their physical temperature (Figure 2).

Figure 2 shows evidence of non-thermal near-IR Emission from an active DAP Phusor, and thermal data, obtained during codeposition. The data is from the DAP Phusor LANR device and an ohmic thermal control. Two pulses are seen representing energy transferred to each in turn. The two inserts show the near-IR outputs of the Phusor and the control over time during each electrical input pulse to each. Below the two insets are some of the thermometry of the DAP codeposition Phusor and an ohmic thermal control.

Excess energy was produced in the pulse on the left side of the figure, after electrical energy was delivered to the DAP Phusor® LANR device. Both thermal output (the pulse in the figure) and near-IR integrated output (inset) of the DAP Phusor® can be seen during its excess energy phase. The pulse on the right side represents electrical energy delivered to a calibrated ohmic thermal control.

Both thermal and near-IR outputs of the DAP Phusor® can be seen during the excess energy phase. Excess energy was produced in the pulse on the left side of the figure, electrical energy delivered to the DAP Phusor®. The pulse on the right side represents electrical energy delivered to a calibrated ohmic thermal control. It can be seen that the dynamic rise of output in the near infrared was only seen in the DAP Phusor® during its activation. By contrast, for the thermal control, despite a higher temperature, there was not an equivalent rising emission observed in the near infrared. The two inserts show the near-IR outputs of the Phusor® and the control over time during each electrical input pulse to each. Below the two insets are some of the thermometry of the DAP codeposition device and an ohmic thermal control.

3.4 Results - Electrohydrodynamic Rayleigh-Bernard instability

We have observed a new phenomenon during codepositional layering of the DAP Phusor cathode. This dynamic instability oscillation, shown in Figure 5, in the voltage-time curves is a dynamic instability, and electrohydrodynamic Rayleigh-Bernard instability associated with the layering (Figure 5). It probably happened like this. First, there was clearing of the ions from the solution, followed by a slow buildup of voltage. Then, increased heating and perhaps other reactions (new carriers, redistribution by bubbling, Bernard instability, new pathways) lead to a sudden hairpin turn, with a fall down of voltage, as the passing the electrical current becomes easier. The time constant was circa 15 minute per cycle, but this was irregularly irregular, with three to five cycles occurring in a 60 minute period.

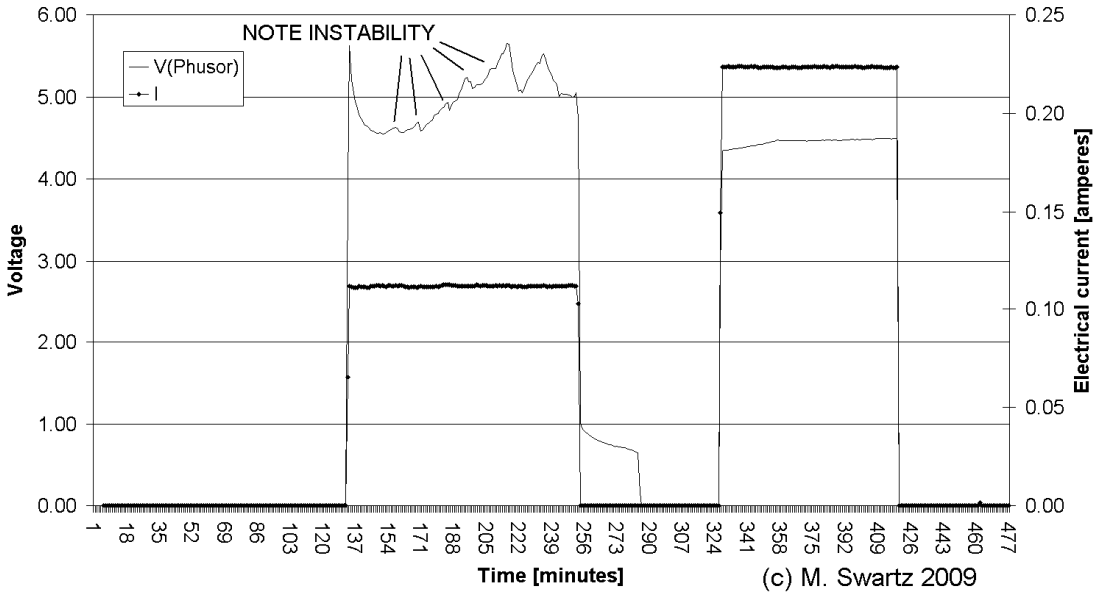

Figure 5- Hydrodynamic instability associated with DAP Phusor® Formation

4. Interpretation and Conclusions

Non-thermal near-IR electromagnetic radiation is emitted from LANR active electrodes when excess heat is observed at their optimal operating point. The appearance of excess energy in several types of high impedance and codeposition Phusor®-LANR (lattice assisted nuclear reaction) devices [Pd high impedance, Pd codeposition, and possibly Ni with light water] was simultaneously detected from loaded, active nickel and palladium devices, by in situ monitoring.

The emission of near-IR from the electrodes when excess heat was only observed when active electrodes operated at their optimal operating point. NT-NIR appears to be linked to, and specific to, a Phusor LANR devices' excess heat production and not its physical temperature. The estimate of the color temperature during NT-NIR of for these LANR devices, driven at their optimal operating point and input power drive levels, was estimated at ~500 to 1000 degrees Kelvin.

In situ near-IR imaging appears to be very useful to monitor LANR cathodes. In addition, information can be obtained by near-infrared superficial reflection spectroscopy. They both may yield information on local loading. However, multi-band in-situ imaging in the visible and near-IR with simultaneous calorimetry is challenging, requiring additional calibrations. We incorrectly thought that the addition of a single control, which was not used by Spzak et al, would be needed. However, as a minimum, actually two controls are needed for examining IR images; thermal controls augmented by spatial controls.

There are several implications of these findings. First, this observation may prove a causative linkage between LANR excess power gain, determined by calorimetry and excess heat flow, and loaded LANR NT-NIR emission.

Second, the observation of non-thermal near-IR synchronous emissions from LANR devices during excess heat production and OOP Operation for palladium and nickel suggests that it might be typical of all Group VIII LANR behavior.

Third, the use of infrared imaging in LANR systems, may be a salient new way to monitor palladium loading.

Fourth, one important implication is that these findings confirm the Bremsstrahlung-shift hypothesis. The Bremsstrahlung-shift hypothesis states that with low temperature fusion, there is a temperature-controlled shift from penetrating ionizing radiation to skin-depth-locked infrared radiation. Because of the much lower temperature, unlike hot fusion or plasma systems, bremsstrahlung radiation in cold fusion systems cannot dissipate fusion derived excess power through penetrating radiation. This temperature difference results in several important changes.

The Bremsstrahlung radiant power density from cold fusion to be markedly lower in intensity, falling from 0.05 - 0.28 (hot fusion) to 1.4 - 8.1 x 10^{-10} for cold fusion. The impact is that the delivered x-ray dose at 1 meter decreases by 11 to 18 orders of magnitude, that is, from 3.1 x 10^{19} Grays (hot fusion) to 1.4 - 3.3 x 10^{-4} Grays for cold fusion. This is consistent with the relative absence of ionizing emissions from most cold fusion systems, except for a few reports looking in the ~6 to 20 keV region. In addition, the temperature difference also causes the output spectrum of the bremsstrahlung radiation to be shifted to the near infra-red.

The impact of this is that these types of energy transfer in cold fusion LANR systems are limited by the skin depth, which for palladium (9.25 x 10^{6} mhos/meter, 10^{13} - 6x10^{14} Hz) is 2.7-20.9 nanometers. The Bremsstrahlung-shift hypothesis [Swartz 1999b] is consistent with, and possibly partially confirmed by, this experimental data in several LANR systems, because the NT-NIR has only been present during excess heat production.

Acknowledgments

The authors thank Larry Parker Forsley, Stan Szpak, Frank Gordon, Pamela Mosier-Boss, Alan Weinberg, Allen Swartz, Alex Frank, Isidor Straus, Steven Olasky, Peter Hagelstein, Brian Ahern, Brian Josephson, Scott Chubb, Raymond Kurzweil, Aaron Kleiner, Charles Entenmann, and Jeffrey Tolleson who have given their critique, support, valued ideas and suggestions, along with JET Energy and the New Energy Foundation for their additional support. PHUSOR® is a registered trademark of JET Energy, Incorporated. Hyperdrive™ and PHUSOR®-technology are protected by U.S. Patents D596724, D413659 and U.S. Patents pending.

REFERENCES

Arata, Y. and Y.C. Zhang (1999)Anomalous Production of Gaseous 4He at the Inside of DS-Cathode During D2-Electrolysis, Proc. Jpn. Acad. Ser. B, Vol. 75, p. 281; Arata, Y. and Y.C. Zhang, Observation of Anomalous Heat Release and Helium-4 Production from Highly Deuterated Fine Particles. Jpn. J. Appl. Phys. Part 2, 1999. 38: p. L774; Arata, Y.

and Y. Zhang, The Establishment of Solid Nuclear Fusion Reactor. J. High Temp. Soc., 2008. 34(2): p. 85

Bass, R.W., M.R.Swartz (2008) Empirical System Identification (ESID) and Optimal Control of Lattice Assisted Nuclear Reaction (LANR) Devices, Proceedings of the 14th International Conference on Condensed Matter Nuclear Science (2010)

Bussard, R.W. (1989) Virtual-State Internal Nuclear fusion in Metal Lattices, Fusion Technology, 16, 231-236

Case, L.C. (1998) Catalytic Fusion of Deuterium into Helium-4. in The Seventh International Conference on Cold Fusion., Vancouver, Canada: Salt Lake City, UT.

Chubb, S.R. and T.A. Chubb (1994) The Role of Hydrogen Ion Band States in Cold Fusion. Trans. Fusion Technol., 26 (4T), 414

Chubb, T.A., S.R.Chubb (1994) Ion Band States: What they are, and How they Affect Cold Fusion, Cold Fusion Source Book, ibid.,75

Cotton, F.A, G.Wilkinson (1972) Advanced Inorganic Chemistry, Interscience, NY

Dardik,I., H. Branover, A. El-Boher, D. Gazit, E. Golbreich, E. Greenspan, A. Kapusta, B. Khachatorov, V. Krakov, S. Lesin, B. Michailovitch, G. Shani, and T. Zilov (2003) Intensification of Low Energy Nuclear Reactions Using Superwave Excitation, Proceedings of the 10th International Conference on Cold Fusion

Dash, J. and D.S. Silver (2007) Surface Studies After Loading Metals With Hydrogen And/Or Deuterium, 13th Conf. CMNS . Sochi, Russia; Dash, J. and S. Miguet, Microanalysis of Pd Cathodes after Electrolysis. J. New Energy, 1996. 1(1): p. 23

Dickson, D.P.E., Berry, F. (1983) Mossbauer Spectroscopy, Cambridge University Press

Fleischmann, M, S. Pons (1989) Electrochemically Induced Nuclear Fusion of Deuterium, J. Electroanal. Chem., 261, 301-308, erratum, 263, 187; M. Fleischmann, S. Pons, Some comments on the paper Analysis of Experiments on Calorimetry of LiOD/D2O Electrochemical Cells, R.H.Wilson et al., J. Electroanal. Chem., 332 (1992)1, J. Electroanal. Chem., 332, 33-53, (1992); M. Fleischmann, S. Pons, Calorimetry of the Pd-D2O system: from simplicity via complications to simplicity, Physics Letters A, 176, 118-129, (1993); M. Fleischmann, S. Pons, M. Anderson, L.J. Li, M. Hawkins, Calorimetry of the palladium-deuterium-heavy water System, Electroanal. Chem., 287, 293, (1990)

Gibb, T.C. (1974) Principles of Mossbauer Spectroscopy, Chapman and Hall, London

Gonser, U (1975) Mossbauer Spectroscopy, Springer-Verlag, NY

Hagelstein, P.L. (1993) Coherent and semicoherent neutron transfer reactions III, Fusion Technol., 23, 353

Hagelstein, P.L., et al. (2008) A Theoretical Formulation for Problems in Condensed Matter Nuclear Science. in ICCF-14 International Conference on Condensed Matter Nuclear Science. Washington, DC.; Hagelstein, P.L. and I. Chaudhary, Models Relevant to Excess Heat Production in Fleischmann-Pons Experiments, in Low-Energy Nuclear Reactions Sourcebook, J. Marwan and S. Krivit, Editors. 2008, Oxford University Press

Hampel, C.A. (1954) Rare Metal Handbook, Reinhold Pub., NY (1954)

Iwamura, Y., M. Sakano, and T. Itoh (2002) Elemental Analysis of Pd Complexes: Effects of D2 Gas Permeation. Jpn. J. Appl. Phys. A, 41: p. 4642; Iwamura, Y., et al., Observation Of Surface Distribution Of Products By X-Ray Fluorescence Spectrometry During D2 Gas Permeation Through Pd Complexes, in The 12th International Conference on Condensed Matter Nuclear Science. 2005. Yokohama, Japan

Kim, Y.E. (2008) Theory of Low-Energy Deuterium Fusion in Micro/Nano-Scale Metal Grains and Particles. Proceedings of the 14th International Conference on Condensed Matter Nuclear Science (2010)

Klein, B.M., R. E. Cohen (1992) Anharmonicity and the inverse isotope effect in the palladium-hydrogen system, Phys. Rev. B, 45, 21, 405

Letts, D. and P.L. Hagelstein (2008) Stimulation of Optical Phonons in Deuterated Palladium. in ICCF-14 International Conference on Condensed Matter Nuclear Science. 2008. Washington, DC.; Letts, D., D. Cravens, and P.L. Hagelstein, Thermal Changes in Palladium Deuteride Induced by Laser Beat Frequencies, in Low-Energy Nuclear Reactions Sourcebook, J. Marwan and S. Krivit, Editors. 2008, Oxford University Press; Letts, D. and D. Cravens. Laser Stimulation Of Deuterated Palladium: Past And Present. in Tenth International Conference on Cold Fusion. (2003)

Letts, D. and D. Cravens (2003) Laser Stimulation of Deuterated Palladium: Past and Present, Proceedings of the 10th International Conference on Cold Fusion

Li, X.Z., et al.(1990) The Precursor of Cold Fusion Phenomenon in Deuterium/Solid Systems. in Anomalous Nuclear Effects in Deuterium/Solid Systems, AIP Conference Proceedings 228. Brigham Young Univ., Provo, UT: American Institute of Physics, NY

McKubre, M., F. Tanzella, P. Hagelstein, K. Mullican, and M. Trevithick (2003) The Need for Triggering in Cold Fusion Reactions, Proc. 10th International Conf. on Cold Fusion

Miles, M.H.,R.A. Hollins, B.F.Bush, J.J. Lagowski, R.E. Miles (1993) Correlation of excess power and helium production during D2O and H2O electrolysis, J. Electroanal. Chem., 346, 99-117; Miles, M.H., B.F.Bush, Heat and Helium Measurements in Deuterated Palladium, Transactions of Fusion Technology, vol 26, Dec. 1994, pp 156-159

Miley, G.H., G. Narne, and T. Woo (2005) Use of combined NAA and SIMS analyses for impurity level isotope detection. J. Radioanal. Nucl. Chem., 263(3): p. 691-696; Miley, G.H. and J. Shrestha, Transmutation Reactions and Associated LENR Effects in Solids, in Low-Energy Nuclear Reactions 2008, Oxford University Press

Mosier-Boss, P.A., Szpak, S. (1999) The Pd/nH System: Transport Processes and Development of Thermal Instabilities, Il Nuovo Cimento, Vol. 112A, pp. 577-585

Mosier-Boss, P.A., Szpak, S., F.E. Gordon, and L.P.G. Forsley (2007) Use of CR-39 in Pd/D Co-Deposition Experiments, European Physics Journal-Applied Physics, Vol. 40, pp. 293-303

Mosier-Boss, P.A., Szpak, S., F.E. Gordon, and L.P.G. Forsley (2009) Triple Tracks in CR-39 as the Result of Pd-D Co-deposition: Evidence of Energetic Neutrons, Naturwissenschaften

Papaconstantopoulos, D.A., B.M. Klein, et alia (1977) Band structure and superconductivity of PdDx and PdHx, Physical Review, 17, 1, 141150

Pons,S., Fleischmann, M. (1994) Heat After Death, Proc. ICCF-4, EPRI TR104188-V2, vol. 2, 8-1; Trans. Fusion Technology, 26, Number 4T, Part 2, p. 87 (December 1994)

Rabinowitz, M., et al. (1993) Opposition and Support for Cold Fusion. in Fourth International Conference on Cold Fusion, Lahaina, Maui: Electric Power Research Institute 3412 Hillview Ave., Palo Alto, CA 94304

Srinivasan, M. et alia., (1992) Tritium and Excess Heat Generation During Electrolysis of Aqueous Solutions of Alkali Salts with Nickel Cathode, Frontiers of Cold Fusion, Ed. by H. Ikegami, Proceedings of the Third International Conference on Cold Fusion, October 21-25, Universal Academy Press, Tokyo, pp 123-138

Stringham, R., (2003) Cavitation and Fusion, ICCF-10. Cambridge, MA

Swartz, M.R.(2008) Three Physical Regions of Anomalous Activity in Deuterided Palladium Mitchell Swartz, Infinite Energy, Vol. 14, Issue 61, 19-3

Swartz, M.R. (1998b) Patterns of Failure in Cold Fusion Experiments, Proceedings of the 33RD Intersociety Engineering Conference on Energy Conversion, IECEC-98-I229, CO

Swartz, M.R. (1997d) Phusons in Nuclear Reactions in Solids, Fusion Technology, 31, 228-

Swartz, M., G. Verner (2009a) Metamaterial Function of Cathodes Producing Hydrogen Energy and Deuteron Flux, Proceedings of the 14th International Conference on Condensed Matter Nuclear Science (2010)
Swartz, M.R. (1997a) Consistency of the Biphasic Nature of Excess Enthalpy in Solid State Anomalous Phenomena with the Quasi-1-Dimensional Model of Isotope Loading into a Material, Fusion Technology, 31, 63-74
Swartz, M. (1996) Possible Deuterium Production From Light Water Excess Enthalpy Experiments using Nickel Cathodes, Journal of New Energy, 3, 68-80
Swartz, M.R. (1997b) Codeposition Of Palladium And Deuterium, Fusion Technology, 32, 126-130
Swartz, M, (1998) Improved Electrolytic Reactor Performance Using -Notch System Operation and Gold Anodes, Transactions of the American Nuclear Association, Nashville, Tenn Meeting, (ISSN:0003-018X publisher LaGrange, Ill) 78, 84-85
Swartz, M.R. (1999a) Generality of Optimal Operating Point Behavior in Low Energy Nuclear Systems, Journal of New Energy, 4, 2, 218-228
Swartz, M.R. (1998) Optimal Operating Point Characteristics of Nickel Light Water Experiments, Proceedings of ICCF-7
Swartz, M.R., G. Verner (2006b) Photoinduced Excess Heat from Laser-Irradiated Electrically-Polarized Palladium Cathodes in D2O, Condensed Matter Nuclear Science, Proc. ICCF-10, eds. Peter L. Hagelstein, Scott Chubb, NJ, ISBN 981-256-564-6, 213-226
Swartz, M.R. (1994a) Isotopic Fuel Loading Coupled to Reactions At an Electrode, Fusion Technology, 26, 4T, 74-77
Swartz, M.R. (1992) Quasi-One-Dimensional Model of Electrochemical Loading of Isotopic Fuel into a Metal, Fusion Technology, 22, 2, 296-300
Swartz, M. (1997c) Noise Measurement in cold fusion systems, Journal of New Energy, 2, 2, 56-61
Swartz, M.R. (2009b) Excess Power Gain and Tardive Thermal Power Generation using High Impedance and Codepositional Phusor Type LANR Devices, Proceedings of the 14th International Conference on Condensed Matter Nuclear Science (2010)
Swartz, M.R., G. Verner (2005) Dual Ohmic Controls Improve Understanding of Heat after Death, Transactions American Nuclear Society, vol. 93, ISSN:0003-018X, 891-892
Swartz, M.R., L.P.Forsley. (2009c) Analysis of Superwave-as-Transitory-OOP-Peak Hypothesis“;Proceedings of the 14th International Conference on Condensed Matter Nuclear Science (2010)
Swartz, M.R., G. Verner (2006a) Excess Heat from Low Electrical Conductivity Heavy Water Spiral-Wound Pd/D2O/Pt and Pd/D2O-PdCl2/Pt Devices, Condensed Matter Nuclear Science, Proceedings of ICCF-10, eds. Peter L. Hagelstein, Scott, R. Chubb, World Scientific Publishing, NJ, ISBN 981-256-564-6, 29-44; 45-54
Swartz, M, G. Verner (1999b) Bremsstrahlung in Hot and Cold Fusion, J New Energy, 3, 4, 90-101
Swartz. M.,P.L.Hagelstein, G. Verner, K. Wright (2003) Transient Vacancy Phase States in Palladium following high dose rate Electron Beam Irradiation, Journal of New Energy
Swartz. M. (1997b) Catastrophic Active Medium Hypothesis of Cold Fusion Vol. 4. Proceedings: Fourth International Conference on Cold Fusion sponsored by EPRI and the Office of Naval Research (1994); Swartz, M., Hydrogen Redistribution By Catastrophic Desorption In Select Transition Metals, Journal of New Energy, 1, 4, 26-33
Swartz. M. (2000b) Patterns of Success in Research Involving Low-Energy Nuclear Reactions, Infinite Energy, 31, 46-48

Swartz. M. (2002) The Impact of Heavy Water (D2O) on Nickel-Light Water Cold Fusion Systems, Proceedings of the 9th International Conference on Cold Fusion (Condensed Matter Nuclear Science), Beijing, China, Xing Z. Li, 335-342

Szpak, S., Mosier-Boss, P.A., S.R. Scharber, and J.J. Smith (1995) Cyclic Voltammetry of Pd+D Codeposition, J. Electroanal. Chem., Vol. 380, pp. 1-6

Szpak, S., Mosier-Boss, P.A., S.R. Scharber, and J.J. Smith (1992) Charging of the Pd/nH System: Role of the Interphase, J. Electroanal. Chem., Vol. 337, pp. 147-163

Szpak, S., Mosier-Boss, P.A., and J.J. Smith (1991) On the Behavior of Pd Deposited in the Presence of Evolving Deuterium, J. Electroanal. Chem., Vol. 302, pp. 255-260

Szpak, S., Mosier-Boss, P.A. (1996) On the Behavior of the Cathodically Polarized Pd/D System: a Response to Vigiers Comments, Phys. Letts. A, Vol. 221, pp. 141-143

Szpak, S., Mosier-Boss, P.A., R.D. Boss, and J.J. Smith (1998) On the Behavior of the Pd/D System: Evidence for Tritium Production, Fusion Technology, Vol. 33, pp. 38-51

Szpak, S., Mosier-Boss, P.A., and J.J. Smith (1994) Deuterium Uptake During Pd-D Codeposition, J. Electroanal. Chem., Vol. 379, pp. 121-127

Szpak, S., et al. (2005) The effect of an external electric field on surface morphology of co-deposited Pd/D films. J. Electroanal. Chem., 580: 284-290

Szpak, S., Mosier-Boss, P.A., and J.J. Smith (1996) On the Behavior of the Cathodically Polarized Pd/D System: Phys. Letts. A, Vol. 210, pp. 382-390

Szpak, S., Mosier-Boss, P.A., C. Young, and F.E. Gordon (2005) Evidence of Nuclear Reactions in the Pd Lattice, Naturwissenschaften, Vol. 92, pp. 394-397

Szpak, S., Mosier-Boss, P.A., M.H. Miles, and M. Fleischmann (2004) Thermal Behavior of Polarized Pd/D Electrodes Prepared by Co-Deposition, Thermochim. Acta, Vol. 410, pp. 101-107

Szpak, S., Mosier-Boss, P.A., and F.E. Gordon (2007) Further Evidence of Nuclear Reactions in the Pd/D Lattice: Emission of Charged Particles, Naturwissenschaften, Vol. 94, 511-514

Takahashi, A. and N. Yabuuchi (2008) Study on 4D/TSC Condensation Motion by Non-Linear Langevin Equation, in Low-Energy Nuclear Reactions Sourcebook, J. Marwan and S. Krivit, Editors. 2008, Oxford University Press; Takahashi, A. Dynamic Mechanism of TSC Condensation Motion. in ICCF-14 International Conference on Condensed Matter Nuclear Science. Washington, DC

Teichler, H. (1991) Theory of hydrogen hopping dynamics including hydrogen-lattice correlations, J. Less-Common Metals, 172-174, 548-556

Violante, V. E. Castagna, C. Sibilia, S. Paoloni, and F. Sarto (2003) Analysis of Mi-Hydride Thin Film After Surface Plasmons Generation by Laser Technique Proceedings of the 10th International Conference on Cold Fusion

Wicke, E., H. Brodowsky (1978) Hydrogen in Palladium and Palladium Alloys, Hydrogen in Metals II, G. Alefield, J. Volkl, Eds., Springer, Berlin

Will, F.G., K. Cedzynska, D.C. Linton (1993) Tritium Generation in Palladium Cathodes with High Deuterium Loading, Transactions of Fusion Technology, vol 26, Dec. 1994, pp 209-213; Reproducible tritium generation in electrochemical cells employing palladium cathodes with high deuterium loading, J. Electroanal. Chem 360, 161-176